PHYSICAL REVIEW B **69**, 094404 (2004)

Electronic structure and magneto-optical Kerr effect in La monochalcogenides

V. N. Antonov* and B. N. Harmon
Ames Laboratory, Iowa State University, Ames, Iowa 50011, USA

A. N. Yaresko
Max Planck Institute for Physics of Complex Systems, D-01187 Dresden, Germany

(Received 3 September 2003; published 11 March 2004)

The optical and magneto-optical (MO) spectra of the lanthanum monochalcogenides are investigated theoretically using the fully relativistic Dirac LMTO band-structure method. The LSDA calculations with shifted La $4f$ empty states describe quite well the shape and magnitude of the LaS MO spectra in an external magnetic field and to a lesser extent the MO spectra of LaSe. On the other hand, theory fails to describe the broader spectral structures in LaTe between 3 and 5 eV. The origin of the Kerr rotation in these compounds is examined.

DOI: 10.1103/PhysRevB.69.094404 PACS number(s): 71.28.+d, 75.30.Mb

I. INTRODUCTION

The trivalent lanthanum monochalcogenides LaS, LaSe, and LaTe possess metallic character having a carrier density in the range of $1.5–2\times10^{22}$ cm^{-3}.[1] The magnetic susceptibility measurements indicate paramagnetism in these compounds.[2] The paramagnetic susceptibility χ_p of conduction electrons has been found to increase from LaS to LaTe suggesting that the density of states at the Fermi energy $N(E_F)$ should also increase from LaS to LaTe. The measured electronic specific-heat coefficient γ also shows the same trend.[3] The Debye temperature θ_D of these compounds is found to decrease from LaS to LaTe.[3] Lanthanum monochalcogenides are found to be superconductors having transition temperatures in the range of 0.8–1.5 K.[3] The superconducting transition temperature T_c increases from sulphide to telluride. A few experimental studies such as point contact spectroscopy,[4] x-ray absorption,[5] and the phonon spectra measurements[6] for LaS are also available in the literature.

The optical and magneto-optical (MO) spectra of LaS, LaSe, and LaTe were investigated in relationship to those of the Ce monochalcogenides by Pittini *et al.*,[7] Pittini and Wachter,[8] and Salghetti-Drioli *et al.*[9] La monochalcogenides are Pauli paramagnets, therefore a nonzero Kerr effect may be obtained only in an external magnetic field. In all three La monochalcogenides a sharp peak in the Kerr rotation was observed, occurring at 3.05, 2.63, and 2.2 eV for LaS, LaSe, and LaTe, respectively. The narrowness of these peaks increases from LaS to LaSe and to LaTe, while the absolute values of the Kerr rotation are 0.99°, 2.54°, and 1.52°, respectively.[9] At higher energies a second broader structure between 4 and 5 eV was observed. This feature is well developed only in LaTe.[9] It was first suggested[7] that the sharp feature in the Kerr rotation is the direct magneto-optical manifestation of an electronic transitions involving empty $4f$ states. Such a claim was based on the fact that its sign was opposite to the one encountered when measuring the Ce-counterpart series.[7] Moreover, the additional line found at about 3 eV was considered as a proof that both $4f^1$ spin-orbit states can be optically populated in contrast to the CeX series, where only the $4f^1$ ground state contributes to the transition.[7,10] However, Salghetti-Drioli *et al.*[9] clearly showed that this is not the case. They found that their spectra present some relevant and essential changes with respect to the previous investigation on LaSe.[7] Even though the peak in the Kerr rotation of LaSe at 2.63 eV is equally sharp in both measurements, the sign is opposite, being negative in the new spectra[9] and positive in Ref. 7. This is due to an incorrect calibration of the spectrometer and particularly to the wrong definition of the magnetic-field direction in the previous investigation.[7] Moreover, for the whole series of compounds Salghetti-Drioli *et al.*[9] do not observe the double peak, found at ≈3 eV in LaSe, as reported in Ref. 7. Salghetti-Drioli *et al.*[9] argue that such a sharp absorption occurs right at the plasma minimum of respective La monochalcogenides and hence the Kerr rotation follows directly from the interplay between optical interband transitions and the plasma resonance.[9] Moreover, they were able to model the situation by applying the phenomenological Lorence-Drude fit. Salghetti-Drioli *et al.*[9] also suggested that the broad absorption developing at higher frequencies between 3 and 5 eV in LaTe is due to interband transitions into empty $4f$ states.

The energy-band structure of lanthanum monochalcogenides have been investigated theoretically in Refs. 11–15 using the LSDA approximation. The calculations have been devoted mostly to investigating the structural properties of La monochalcogenides. The total energy calculations for lanthanum monochalcogenides reported in Ref. 15 underestimate the experimental value of lattice constant by 1.9, 1.68, and 2.3 % in LaS, LaSe, and LaTe, respectively. The corresponding bulk modulus is overestimated when compared to the experimental data by 24% and 35% in LaS and LaTe, respectively. The electronic structure of LaS and the LaS/CdS interface have been studied in Ref. 14. The observed low work function of LaS is well reproduced by the LSDA theory. As far as we know, there are no first-principles theoretical investigations of the optical and MO properties of La monochalcogenides in the literature.

The aim of this work is the theoretical study of the electronic structure, optical, and magneto-optical spectra of LaS, LaSe, and LaTe in an external magnetic field. The paper is organized as follows. Section II presents a description of the crystal structure of the lanthanum monochalcogenides and computational details. Section III is devoted to the electronic structure, optical, and MO properties of LaS, LaSe, and LaTe. The optical and MO theoretical calculations are compared to the experimental measurements. Finally, the results are summarized in Sec. IV.

II. CRYSTAL STRUCTURE AND COMPUTATIONAL DETAILS

All the three chalcogenides, namely LaS, LaSe, and LaTe, considered in the present work crystallize in the NaCl type structure ($B1$) with space-group symmetry $Fm3m$. The lanthanum atom is positioned at (0, 0, 0) and the chalcogen atom at (1/2, 1/2, 1/2).

The details of the computational method are described in our previous papers,[16,17] and here we only mention several aspects. The calculations were performed for the experimentally observed lattice constants $a=5.86$, 6.06, and 6.436 Å. We used the von Barth–Hedin parametrization[18] for the exchange-correlation potential. Brillouin zone integrations were performed using the improved tetrahedron method[19] and charge self-consistency was obtained with 1330 irreducible **k** points. To improve the potential we include additional empty spheres in the (1/4, 1/4, 1/4) positions. The basis consisted of La s, p, d, f, and g; chalcogen s, p, and d LMTO's. The combined correction terms have been included also in calculation of the optical matrix elements.[20] We have calculated the absorptive part of the optical conductivity in a wide energy range. The Kramers-Kronig transformation has been used to calculate the dispersive parts of the optical conductivity from the absorptive parts.

It is known that magneto-optical phenomena reflect the electronic states of the spin polarized band structure and arise due to simultaneous occurrence of the exchange splitting and spin-orbit coupling. La monochalcogenides are Pauli paramagnets and a nonzero exchange splitting may be obtained only in an external magnetic field. To calculate the electronic structure and MOKE spectra of paramagnetic La monochalcogenides, the term $2\mu_B\vec{B}\cdot\vec{s}$ which couples the spin of the electron to the external magnetic field was added to the Hamiltonian at the variational step, and the self-consistent solution was obtained.

The application of standard LSDA methods to f-shell systems meets with problems in most cases, because of the correlated nature of the f electrons. There are actually different attempts to improve the LSDA to treat correlated electrons: GW approach, Dynamical mean-field theory, time-dependent density-functional theory, self-interaction correction, and LSDA+U method being the most used ones.[21] To model the effect of "self-magnetic" impurity (see below) on the electronic structure and MO properties, we have adopted as a suitable model Hamiltonian that of the LSDA+U approach.[22,23] In our LSDA+U calculations the screened Coulomb U and exchange J integrals between different orbitals were assumed to be of equal to their averaged values. In this approximation the effective one-electron LSDA+U potential $V_{m\sigma}^{\mathrm{LSDA}+U}=V^{\mathrm{LSDA}}+U_{eff}(1/2-n_{m\sigma})$ is determined by $U_{eff}=U-J$ and orbital occupation numbers $n_{m\sigma}$. We set the U_{eff} to 6.0 eV. In principle, U_{eff} can be determined from constrained LSDA calculations. However, the calculated value of U_{eff} depends on theoretical approximations and for our purposes it is sufficient to regard the value of U_{eff} as an adjustable parameter and try to ascertain its value from comparison of the calculated physical properties of La monochalcogenides with experiments. We found that the optical and MO spectra are rather insensitive to the precise value of U_{eff}. The LSDA+U band-structure calculations with U_{eff} varying from 4 to 6 eV provide the optical and MO spectra in a reasonable agreement with the experimental data.

Hubbard U_{eff} takes into account the Coulomb correlations between $4f$ electrons. In the process of self-consistent LSDA+U band-structure calculations occupied $4f$ states are shifted downward by $U_{eff}/2$ and empty levels are shifted upwards by the same amount. One should mention, however, that La monochalcogenides have no occupied $4f$ electrons, therefore the direct application of the LSDA+U method is problematic conceptually in this case. To put the La empty $4f$ energy states in right position, we add a constant potential to the Hamiltonian which acts only on the $4f$ states. This potential shifts the fourteen on-site $4f$ energies upwards by about 3 eV. We emphasize, however, that the $4f$ states are hybridized, and together with all other states their energy positions relax to self consistency. Numerically this procedure is equivalent to using of the LSDA+U method with $U_{eff}=6.0$ eV.

III. RESULTS AND DISCUSSION

A. Electronic structure

Figure 1 shows the fully relativistic energy band structure of LaS calculated in an external magnetic field. In these calculations the $4f$ states have been considered as: (1) itinerant using the local spin-density approximation and (2) fully localized, treating them as core states, but unoccupied. The energy band structure of LaS without the $4f$ states can be subdivided into three regions separated by energy gaps. The bands in the lowest region around -15 to -13.5 eV have mostly S s character with some amount of La sp character mixed in. The next six energy bands are S p bands separated from the s bands by an energy gap of about 7 eV. The width of the S p band is about 3.7 eV. The spin splitting of the S p bands is very small [about 0.03 eV at the X symmetry point (Fig. 1)]. The highest region can be characterized as La spin-split d bands. La E_g d states are shifted toward higher energy due to hybridization with S p states. It is important that the top of the S p bands is at -2.8 eV below the Fermi level, since it means that all the interband transitions in the energy interval of 0.0–2.8 eV take part within the La d bands (see below). The LSDA calculations place the empty $4f$ states of La in LaS at 1–2 eV above the Fermi level. It is well known that LSDA usually gives a wrong energy position for the $4f$ states in rare-earth compounds. For nonzero $4f$ occupation it places the $4f$ states right at the Fermi level[16,17] in contradiction with various experimental observations. In the case of La compounds the LSDA places the empty $4f$ states too

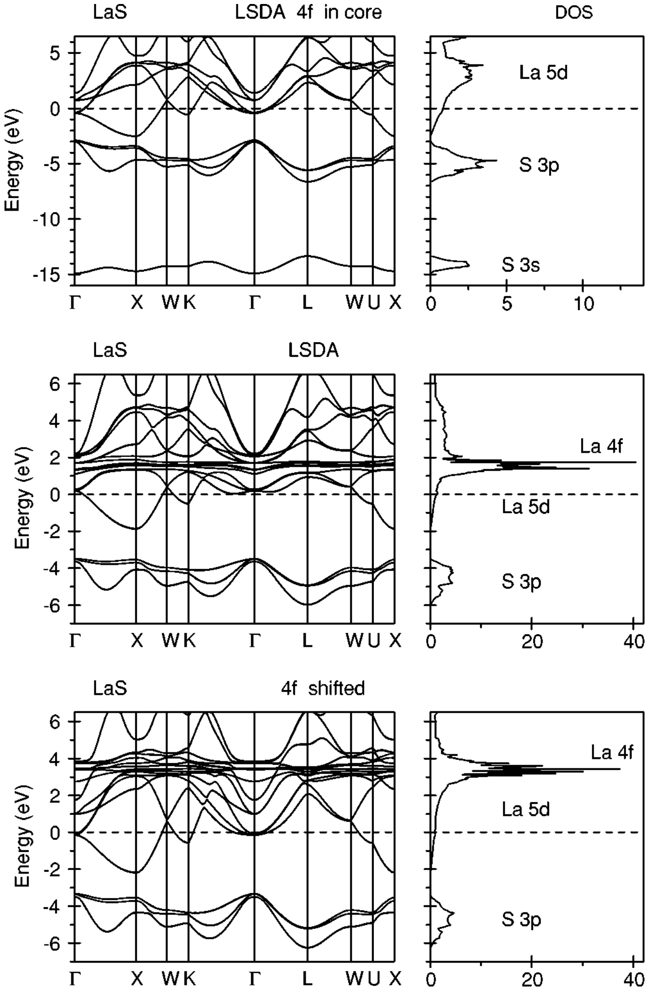

FIG. 1. Self-consistent fully relativistic energy-band structure and total DOS [in states/(unit cell eV)] calculated with external magnetic field of 60 T for LaS.

close to the Fermi energy. For example, the LSDA calculations produce the empty $4f$ states in pure La metal at 2.7 eV above the Fermi level,[24] although according to the BIS measurements they are situated around 5.5 eV above the Fermi level.[25,26] To put the La empty $4f$ energy states in right position we add a constant potential of 3 eV to the Hamiltonian which acts only on the $4f$ states. Figure 1 presents the energy band structure of LaS calculated with shifted $4f$ states. In such an approximation the La $4f$ empty states are situated around 3.5 eV above the Fermi level. Besides the upward shift of the La $4f$ states there are some other minor changes in the band structure, namely, the empty La $5d$ states at the Γ symmetry point in the LSDA calculations become occupied in the approximation with shifted $4f$ states (Fig. 1).

Figure 2 shows the energy band structure and total density of states (DOS) of LaSe and LaTe using an additional constant potential acting on the $4f$ states with the same value as was used for LaS. The main trend in the electronic structure of the sequence of LaX compounds (X = S, Se, or Te) results from the characteristic trend in the chalcogenide p and d wave functions and from the systematic change of the lattice parameters. The counteraction of screening by inner atomic shells and of relativistic effects leads to the characteristic trend in the position of the atomic p state and hence of the center of gravity of the chalcogenide p band, increasing from S to Te. The p bandwidth is monotonically increasing from S to Te due to the increasing extension of the atomic np wave function, although the lattice constant increases too. The direct energy gap between chalcogenide p and d bands decreases from LaS to LaTe (Fig. 2). The center of gravity of unoccupied $4f$ bands situated at 3.4, 3.2, and 2.9 eV above the Fermi level in LaS, LaSe, and LaTe, respectively. The degree of localization of La $4f$ states in the LaS-LaSe-LaTe row is increased due to increasing of La-La interatomic distances. The $4f$ states became narrower and besides are shifted toward the Fermi level in going from LaS to LaTe (see Figs. 1 and 2).

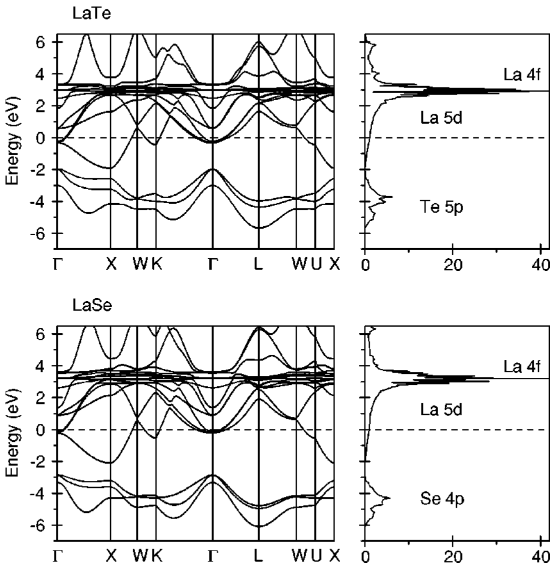

FIG. 2. Self-consistent fully relativistic energy-band structure and total DOS [in states/(unit cell eV)] calculated for LaSe and LaTe in an external magnetic field of 60 T with shifted $4f$ states.

B. Optical spectra

Figure 3 shows the calculated diagonal part of the optical conductivity σ_{1xx} and the optical reflectivity R of LaS, LaSe, and LaTe in the LSDA and with shifted $4f$ states approximations compared with the experimental data.[7,9] The calculated spectra have been convoluted with a Lorentzian whose width is 0.3 eV to approximate a lifetime broadening. The most prominent discrepancy in optical conductivity spectra calculated using the conventional LSDA approximation is the extra peak situated at 2.3 and 2.1 eV in LaS and LaSe, respectively (Fig. 3). The corresponding structure is less pronounced in the case of LaTe. This peak is caused by extra structure present in the interband dielectric tensor. Responsible are interband transitions involving the hybridized empty $4f$ states, which in the LSDA approach exhibit a resonance too close to the Fermi energy. The peak is also responsible for the minimum in the optical reflectivity in LaS and LaSe at around 2.0 eV which is not observed in the experiment (Fig. 3). In the calculations with shifted $4f$ states the

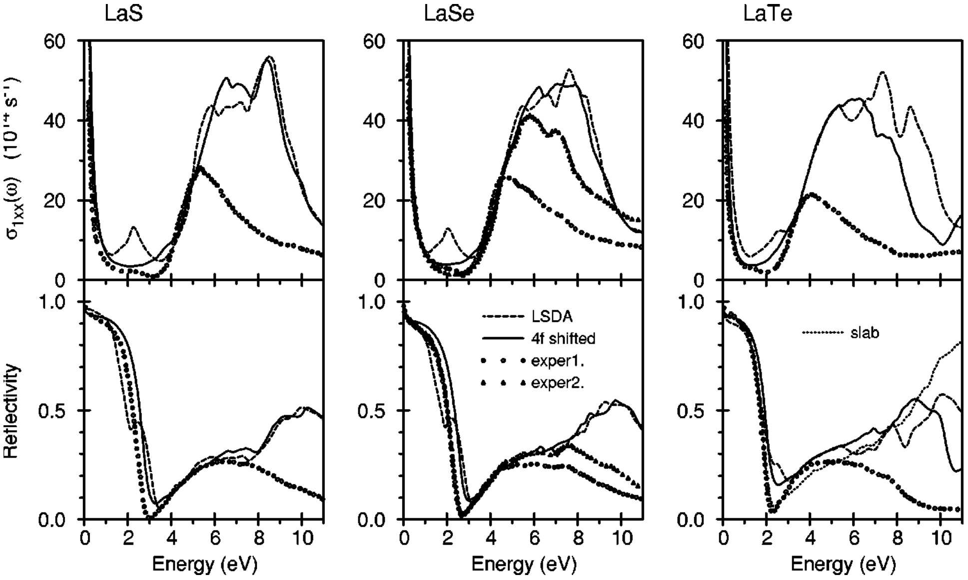

FIG. 3. Calculated diagonal part of the optical conductivity σ_{1xx} and the optical reflectivity R of LaS, LaSe, and LaTe in the LSDA (dotted line) and with shifted $4f$ states (solid line) compared with the experimental data Ref. 9 (circles) and Ref. 7 (triangles). There optical reflectivity spectrum of LaTe calculated for a 5/3 multilayered structure (slab) is also shown (see the explanation in the text).

transitions involving the $4f$ states do not take place at small photon energies any more, and the erroneous peak structure disappears from optical conductivity spectra.

On the basis of the results of the band-structure calculations of lanthanum monochalcogenides, their observed optical reflectivity spectra (Fig. 3) can be sorted into the respective interband transition groups: (1) metallic high reflectivity below ~2 eV, (2) a steep edge between ~2 and ~2.5 eV, and (3) above a minimum at ~2.7 eV some less pronounced structures with a broad maximum of R between 5 and 9 eV mostly caused by $3p \rightarrow 5d$ interband transitions.

The predominant structure of the lanthanum monochalcogenides spectra is the edge at 2.9, 2.7, and 2.3 eV in LaS, LaSe, and LaTe, respectively. This sudden drop is characteristic for metallic rare-earth chalcogenides and is due to a plasma oscillation interfering with interband excitations.[27] The energy of the conduction-electron plasma resonance in the presence of the interband excitations is given by $\varepsilon_{1xx}(\omega)=0$.

We should mention one important discrepancy between the theory and the experiment. Namely, the edge in the optical reflectivity spectra which is caused by the plasma oscillations is deeper in the experimental spectra in comparison with the theoretically calculated one for all the three compounds. One of the possible reasons may be the influence of the surface. To model the surface effects, we carried out band-structure calculations using a tetragonal supercell containing four unit cells of LaTe along z direction in which three LaTe layers are replaced by three layers of empty spheres. The optical reflectivity spectrum of LaTe calculated for such a five layer slab separated by three layers of empty spheres [5/3 multilayered structure (MLS)] is in excellent agreement with the experimental measurements (Fig. 3). We also carried out the band-structure calculations for a nine layer slab separated by three layers of empty spheres (9/3 MLS) which give results similar to those for 5/3 MLS.

Above 5 eV the theoretically calculated optical conductivity and reflectivity spectra of lanthanide monochalcogenides are larger in comparison with the experimental measurements. One of the possible reasons for this is a nonideal sample surface, its roughness can reduce the optical reflectivity above 5 eV. As a result the experimental optical conductivity spectrum which has been derived from the reflectivity data through the Kramers-Kronig transformation has a lower intensity in comparison with the theoretical calculations (Fig. 3). We present two experimental measurements of the optical reflectivity in the case of LaSe in Fig. 3. It is clearly seen that even small deviation in the optical reflectivity spectra above 5 eV causes a great difference in the absolute value of the optical conductivity spectrum.

C. MO spectra

After consideration of the band structure and optical properties we turn to the magneto-optical spectra. In the polar geometry, where the z axis is chosen to be perpendicular to the solid surface, and parallel to the magnetization direction, the expression for the Kerr angle can be obtained easily for small angles and is given by[28]

$$\theta_K(\omega)+i\varepsilon_K(\omega)=-\sigma_{xy}(\omega)/D(\omega), \tag{1}$$

where

$$D(\omega)=\sigma_{xx}(\omega)\sqrt{1+\frac{4\pi i}{\omega}\sigma_{xx}(\omega)}, \tag{2}$$

with θ_K the Kerr rotation and ε_K the so-called Kerr ellipticity. $\sigma_{\alpha\beta}$ $(\alpha,\beta\equiv x,y,z)$ is the optical conductivity tensor, which is related to the dielectric tensor $\varepsilon_{\alpha\beta}$ through

$$\varepsilon_{\alpha\beta}(\omega)=\delta_{\alpha\beta}+\frac{4\pi i}{\omega}\sigma_{\alpha\beta}(\omega). \tag{3}$$

In Fig. 4 we show the experimental[9] $\theta_K(\omega)$ and $\epsilon_K(\omega)$ MO Kerr spectra of LaS, as well as the spectra calculated with the LSDA, the $4f$ states in the core and the LSDA with

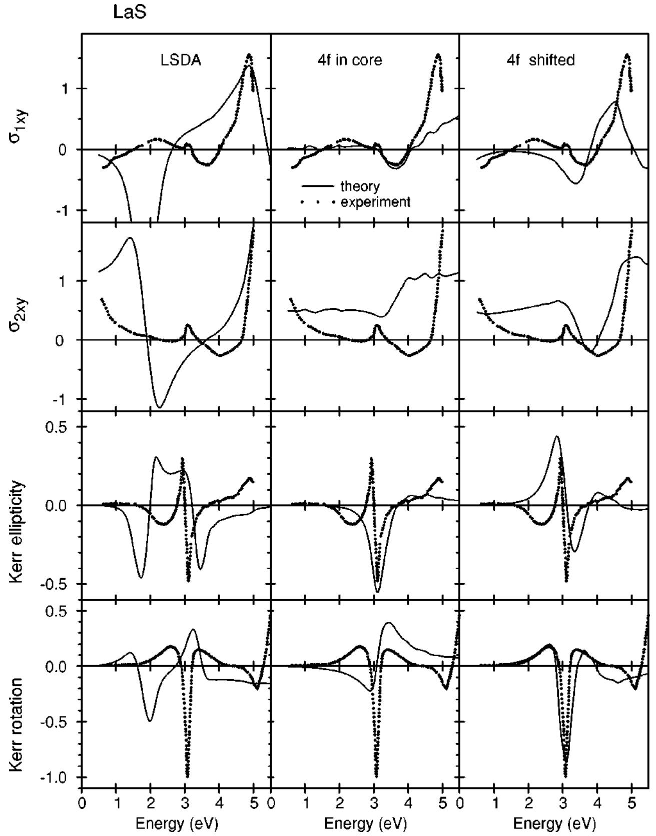

FIG. 4. Calculated off-diagonal parts of the dielectric function ε_{xy} (in 10^{29} s^{-2}), Kerr rotation and Kerr ellipticity spectra (in degree) for LaS treating the $4f$ states as a core electrons, LSDA and LSDA with shifted $4f$ states compared with experimental data (circles) (Ref. 9).

shifted $4f$ states. This picture clearly demonstrates that the best description is given by the LSDA approach with shifted $4f$ states.

Due to the wrong position of the $4f$ bands in conventional LSDA calculations the off-diagonal part of the dielectric function ε_{xy} displays additional resonance structures at 1.0 and 2.4 eV, which leads to a disagreement with the experimental Kerr spectra. The most prominent discrepancy in the LSDA Kerr rotation and ellipticity spectra is the negative peak at around 2 eV which is caused by the $5d \rightarrow 4f$ interband transitions. In the LSDA approach with shifted $4f$ states the transitions involving the $4f$ states do not take place at these photon energies any more, and the erroneous peak structure around 2 eV disappears from Kerr spectra. The calculations in which the $4f$ states are treated as quasicore are also not able to reproduce the correct MO spectra of LaS.

The LSDA calculations with shifted $4f$ states produce a single resonance minimum in the Kerr rotation spectrum in good agreement with the experimental measurements. The theoretical analysis of separate contributions of both the numerator, i.e., $\sigma_{xy}(\omega)$ and the denominator, $D(\omega)$ [Eq. (2)], which factor together to give the Kerr angle shows that the shape of the Kerr ellipticity and Kerr rotation spectra in this compound are almost completely determined by the shape of the function $[\omega \mathrm{D}(\omega)]^{-1}$. Off-diagonal $\sigma_{1xy}(\omega)$ and $\sigma_{2xy}(\omega)$ optical conductivity of LaS calculated in the LSDA approximation with shifted $4f$ states show almost constant energy behavior below 3 eV. Figure 5 shows the theoretically calculated Kerr rotation and ellipticity of LaS and the frequency dependence of real and imaginary parts of the function $[\omega \mathrm{D}(\omega)]^{-1}$ multiplied by a constant to normalize the spectra. Obviously the shape of the Kerr spectra in LaS results mostly from the resonance structure of the function $[\omega \mathrm{D}(\omega)]^{-1}$ below 3 eV. Although above this energy the shape of the Kerr spectra is determined by the interplay between optical interband transitions and the plasma resonance.

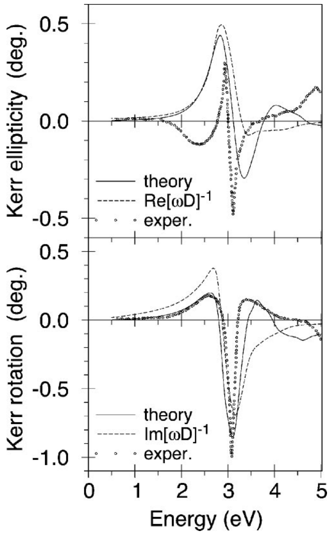

FIG. 5. Calculated Kerr rotation and Kerr ellipticity spectra (in degree) for LaS in an external magnetic field of 60 T compared with experimental data (Ref. 9). The real and the imaginary parts of the function $[\omega \mathrm{D}(\omega)]^{-1}$ are also shown.

A similar situation is observed in the case of LaSe. The best description of the Kerr spectra of LaSe is given by the LSDA approach with shifted $4f$ states (Fig. 6). The resonance structure observed in the Kerr rotation spectrum is

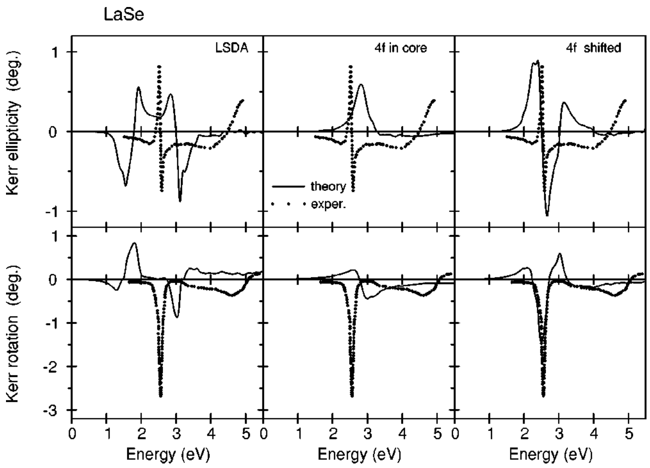

FIG. 6. Calculated Kerr rotation and Kerr ellipticity spectra (in degree) for LaSe in an external magnetic field of 60 T treating the $4f$ states as a core electrons, conventional LSDA and LSDA with shifted $4f$ states compared with experimental data (circles) (Ref. 9).

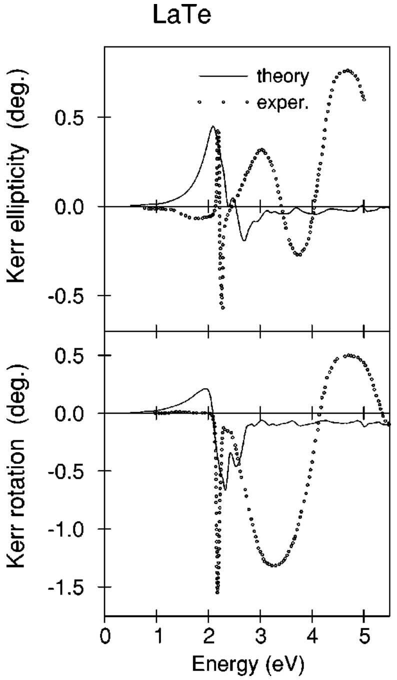

FIG. 7. Calculated Kerr rotation and Kerr ellipticity spectra (in degree) for LaTe in an external magnetic field of 60 T compared with experimental data (circles) (Ref. 9).

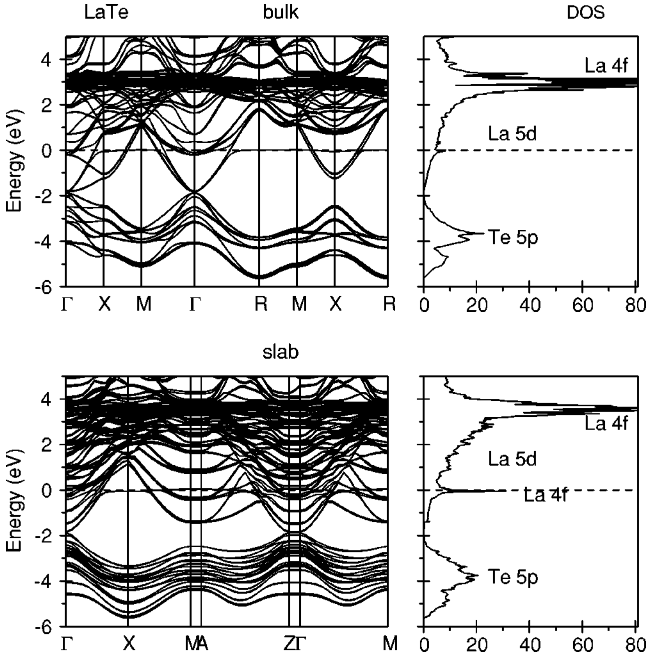

FIG. 8. The energy-band structure and total DOS [in states/(unit cell eV)] of LaTe calculated in a supercell for bulk and slab approximations with one of the La atoms having a $4f^1$ occupation (see the explanation in the text).

mostly determined by the resonance structure of the function $[\omega \mathrm{D}(\omega)]^{-1}$. Although the high-energy part of the Kerr spectra is affected also by the optical interband transitions.

Figure 7 shows the experimental[9] $\theta_K(\omega)$ and $\epsilon_K(\omega)$ MO Kerr spectra of LaTe, as well as the spectra calculated in the LSDA approximation with shifted $4f$ states. Theory gives a much smaller resonance structure in the Kerr rotation spectrum and fails to produce a broader structure observed experimentally at higher energies between 3 and 5 eV.[9] This feature is well recognized only in LaTe. Salghetti-Drioli *et al.*[9] suggested that the broad absorption developing between 3 and 5 eV is due to interband transitions into empty $4f$ states. In our band-structure calculations the center of gravity of empty $4f$ energy bands is shifted downwards by 0.4 eV going from LaSe to LaTe (Fig. 2). So a similar broad absorption in the Kerr rotation spectrum might be expected to be observed in LaSe starting at around 3.5 eV. Although there is a negative peak in the Kerr rotation spectrum of LaSe it occurs near 4.7 eV (Fig. 6) and has a much smaller intensity in comparison with the corresponding structure in LaTe.

There is another important discrepancy between the theory and the experiment. The MO measurements of lanthanum monochalcogenides[9] were performed in external magnetic fields up to 13.2 T. On the other hand, to achieve the same absolute value of the Kerr rotation in LaS and LaSe we used in our calculations an external magnetic field of 60 T. In other words, to achieve the same Zeeman splitting we need to use 5 times larger external magnetic field in comparison with the experimental conditions. The effective increase of the magnetic field may be caused by some amount of magnetic impurities. We can also imagine another, so called "self-magnetic" impurity mechanism. The ground state of lanthanum monochalcogenides have empty $4f$ states. The light absorption in the optical measurements leads to excited states of the La atom, which may include $5d \rightarrow 4f$ interband electron transitions. The exited electron in $4f$ state may exist quite a long time on the same site depending on the degree of the localization of the $4f$ states in the compound. Such a $4f^1$ configuration decays to the ground state most probably through the Auger process emitting an addition electron from valence band. Due to energy balance it might be La d electron. An additional hole in d valence band will not influence the optical spectra due to its small lifetime.

To model the situation we carried out two supercell band-structure calculations using the LSDA+U approximation with $U_{eff}=6$ eV. In the first calculations we used four unit cells in which one of four La atoms has a $4f^1$ configuration. The second calculations have been carried out for 5/3 MLS with a five layered slab separated by three layers of empty spheres. For the surface La (first and fifth layers) we used a $4f^1$ configuration and for the other three layers a $4f^0$ configuration. The corresponding band structures and total DOS for LaTe are presented in Fig. 8. We found a ferromagnetic self-consistent solutions with the spin, orbital, and total magnetic moments equal to $-0.455\mu_B$, $1.285\mu_B$, and $0.830\mu_B$, and $-0.658\mu_B$, $1.815\mu_B$, and $1.157\mu_B$ for the La site with a $4f^1$ configuration in the bulk and slab, respectively. One should note also that the empty La $4f$ states of the surface layer are shifted toward E_F at around 0.5 eV in comparison with the bulk calculations. The partly occupied $4f^1$ state is strongly hybridized with La 5d states and pinned to the Fermi level in both the calculations. The reduction of the number of neighbors of an atom located at the surface

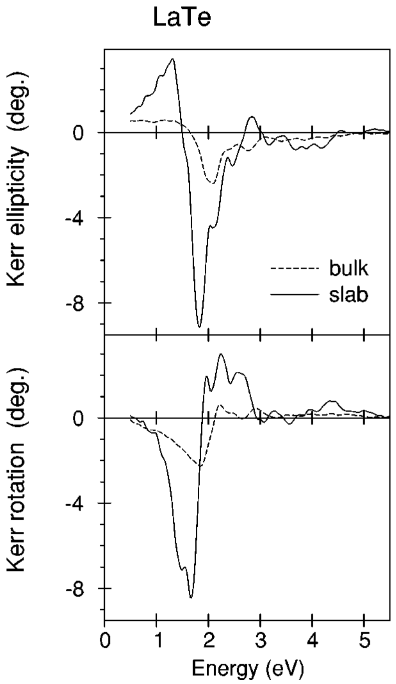

FIG. 9. Kerr rotation and Kerr ellipticity spectra (in degree) of LaTe calculated in supercell approximation for bulk and slab approximations with one of La atoms having a $4f^1$ occupation (see the explanation in the text).

decreases its hybridization and, as a consequence, the width of this (possible) surface state substantially decreases in comparison with the bulk state. A half width of a $4f^1$ state is equal to 0.04 and 0.10 eV for surface and bulk La atoms, respectively.

The existence of the occupied $4f^1$ state leads to a strong polarization of the system. Figure 9 presents the Kerr rotation and ellipticity spectra calculated for the super-cell bulk approximation and for the 5/3 MLS. It can be seen that such a ‘‘self-magnetic’’ impurity mechanism increases the absolute value of the Kerr rotation for LaTe by four times in the bulk and by one order of magnitude for the slab.

One should mention that the corresponding partly occupied $4f^1$ level appears only in constrained LSDA+U calculations in which the occupation of one of La $4f$ states ($m_j = -5/2$) was fixed to 1. If the orbital occupation numbers were allowed to relax LSDA+U calculations resulted in $4f^0$ configuration. Although the solution with partly occupied La $4f$ state can be obtained only in the constrained LSDA+U calculations, the occupation number of the pinned $4f^1$ level after self-consistent procedure is closer to 1 for the surface La atom in comparison with the bulk one. Therefore the probability of the existing of the self-magnetic impurity mechanism is larger for a surface atoms.

This mechanism may explain why in our band-structure calculations we need to increase the value of the external magnetic field up to five times in comparison with the experimental conditions. Although our supercell band-structure calculations still do not produce the broad absorption between 3 and 5 eV in the MOKE spectra of LaTe (Fig. 7). The situation might be similar to that for CeSb, where the record Kerr rotation of 90° was observed.[29] Later on Salghetti-Drioli *et al.*[30] prepared well-characterized single crystals of CeSb, but could not reproduce the record Kerr rotation on a new crystal. Instead only a peak of −17° was observed. Salghetti-Drioli *et al.* suggest that the observed 90° Kerr rotation might not be the intrinsic rotation of CeSb, but could be caused by a surface oxide layer. Possibly a similar situation is also happening in the case of LaTe.

IV. SUMMARY

The LSDA calculations with shifted La $4f$ empty states reasonably describe the shape and magnitude of the optical and MO spectra in LaS in an external magnetic field and to a less extent the MO spectra in LaSe. The theoretical analysis of separate contributions of both the numerator, i.e., $\sigma_{xy}(\omega)$ and the denominator, $D(\omega)$ of the Kerr rotation and ellipticity spectra shows that their shape in La monochalcogenides are almost completely determined by the shape of the function $[\omega \mathrm{D}(\omega)]^{-1}$ below 3 eV. This conclusion just confirms the idea already drawn by Salghetti-Drioli *et al.*[9] that the sharp Kerr effect in lanthanum monochalcogenides follows directly from the interplay between an optical interband transitions and the plasma resonance.

The edge in the optical reflectivity spectra in La chalcogenides are deeper and the corresponding Kerr rotation spectra have narrower resonance structures in the experimental spectra in comparison with the theoretically calculated ones. One possible reason is the influence of surface effects.

To achieve the same absolute value of the Kerr rotation in LaS and LaSe we must use in our calculations an external magnetic field five times larger than the experimental one. This might be associated with possible creation of La f^1 surface states which cause an additional polarization of the system.

Theory fails to describe the broader structures in the MO spectra of LaTe between 3 and 5 eV. These structures might not be associated with the intrinsic rotation of LaTe, but could be caused by some additional surface structures. To clarify the nature of these features a new series of MO experiments with special attention to the surface conditions are highly desired.

ACKNOWLEDGMENTS

This work was carried out at the Ames Laboratory, which is operated for the U.S. Department of Energy by Iowa State University under Contract No. W-7405-82. This work was supported by the Director for Energy Research, Office of Basic Energy Sciences of the U.S. Department of Energy. The authors gratefully acknowledge a valuable discussion with Professor Yu. N. Kucherenko.

---

[*] Permanent address: Institute of Metal Physics, Vernadsky Street, 03142 Kiev, Ukraine. Email address: antonov@ameslab.gov; anton@imp.kiev.ua

[1] V.P. Zhuze, M.G. Karin, D.P. Lukirskii, M. Sergeeva, and A.I. Shelykh, Fiz. Tverd. Tela (Leningrad) **22**, 2669 (1980) [Sov. Phys. Solid State **22**, 1558 (1980)].

[2] V.E. Adamyan, N.P. Bodrova, E.V. Goncharova, and G.M. Loginov, Fiz. Tverd. Tela (Leningrad) **12**, 2239 (1971) [Sov. Phys. Solid State **22**, 2239 (1980)].

[3] E. Bucher, K. Andres, F.J. di Salvo, J.P. Maita, A.C. Gossard, A.S. Cooper, and G.W. Hull, Phys. Rev. B **11**, 500 (1975).

[4] I. Frankauski and P. Wachter, Solid State Commun. **40**, 885 (1998).

[5] W. Beckenbauch, J. Evers, G. Gunterhof, E. Kaldis, and J. Watcher, J. Phys. Chem. Solids **36**, 239 (1975).

[6] M.M. Steiner, H. Eschrig, and R. Monnier, Phys. Rev. B **45**, 7183 (1992).

[7] R. Pittini, J. Schoenes, F. Hulliger, and P. Wachter, Phys. Rev. Lett. **78**, 725 (1977).

[8] R. Pittini and P. Wachter, J. Magn. Magn. Mater. **177-181**, 1025 (1988).

[9] F. Salghetti-Drioli, P. Wachter, and L. Degiorgi, Solid State Commun. **109**, 773 (1999).

[10] R. Pittini, J. Schoenes, and P. Wachter, Phys. Rev. B **55**, 7524 (1997).

[11] S.V. Vlasov and O.V. Farberovich, Solid State Commun. **56**, 967 (1985).

[12] Z.W. Lu, D.J. Singh, and H. Krakauer, Phys. Rev. B **37**, 10 045 (1988).

[13] S. Sankapalingam, S.M. Jaya, G. Pari, and R. Asokamani, Phys. Status Solidi B **174**, 435 (1992).

[14] O. Eriksson, J. Wills, P. Mumford, M. Cahay, and W. Friz, Phys. Rev. B **57**, 4067 (1998).

[15] G. Vaitheeswaran, V. Kanchana, and M. Rajagopalan, J. Phys. Chem. Solids **64**, 15 (2003).

[16] V.N. Antonov, B.N. Harmon, and A.N. Yaresko, Phys. Rev. B **63**, 205112 (2001).

[17] V.N. Antonov, B.N. Harmon, and A.N. Yaresko, Phys. Rev. B **66**, 165208 (2002).

[18] U. von Barth and L. Hedin, J. Phys. C **5**, 1629 (1972).

[19] P.E. Blöchl, O. Jepsen, and O.K. Andersen, Phys. Rev. B **49**, 16 223 (1994).

[20] V.N. Antonov, A.I. Bagljuk, A.Y. Perlov, V.V. Nemoshkalenko, Vl.N. Antonov, O.K. Andersen, and O. Jepsen, Low Temp. Phys. **19**, 494 (1993).

[21] V.V. Nemoshkalenko and V.N. Antonov, *Computational Methods in Solid State Physics* (Gordon and Breach Science Publication, Amsterdam, 1998).

[22] V.I. Anisimov, J. Zaanen, and O.K. Andersen, Phys. Rev. B **44**, 943 (1991).

[23] A.N. Yaresko, V.N. Antonov, and P. Fulde, Phys. Rev. B **67**, 155103 (2003).

[24] W.E. Picket, A.J. Freeman, and D.D. Koelling, Phys. Rev. B **22**, 2695 (1980).

[25] J. Lang, Y. Baer, and P. Cox, J. Phys. F: Met. Phys. **11**, 121 (1981).

[26] Y. Baer and W.D. Schneider, in *Handbook of the Physics and Chemistry of Rare Earths*, edited by K.A. Gschneidner, L. Eyring, and S. Hüfner (North-Holland, Amsterdam, 1987), Vol. 10, p. 1.

[27] B. Batlogg, Phys. Rev. B **23**, 1827 (1981).

[28] W. Reim and J. Schoenes, in *Ferromagnetic Materials*, edited by E.P. Wohlfarth and K.H.J. Buschow (North-Holland, Amsterdam, 1990), Vol. 5, p. 133.

[29] R. Pittini, J. Schoenes, O. Vogt, and P. Wachter, Phys. Rev. Lett. **77**, 944 (1996).

[30] F. Salghetti-Drioli, K. Mattenberger, P. Wachter, and L. Degiorgi, Solid State Commun. **109**, 687 (1999).